



## I. INTRODUCTION

The discovery of the accelerating expansion of the Universe was performed by observations of distant Type Ia Supernovae (SNe Ia) [1, 2] and caused a resurgence of interest for this type of astrophysical transients. It turns out that in the last two decades the discovery rate of SNe Ia has been dramatically increased. The future projects such as the Vera C. Rubin Observatory Legacy Survey of Space and Time [3] will provide even more observations of this phenomenon and allow us to measure the cosmological parameters with the highest accuracy.

Cosmological parameters are estimated from the “luminosity distance-redshift” relation of SNe Ia using the Hubble diagram. Currently, a lot of attention is paid to enhance the accuracy of SN luminosity standardisation [4]. The other effect that decreases the accuracy of the luminosity distance measurements is the gravitational lensing. In [5] the authors showed that its contribution at the low redshifts is negligible but increases with the redshift growth.

The uncertainty on the redshift in the “luminosity distance-redshift” relation is quite often considered negligible. In this relation, the redshift  $z$  should be entirely due to the expansion of the Universe, i. e. relative to the CMB frame. However, the observed redshift  $z_{obs}$  contains a contribution from the poorly known peculiar velocities:  $(1 + z_{obs}) = (1 + z)(1 + z_{pec})$ , where  $z_{pec}$  corresponds to the peculiar velocity  $v_{pec}$  contribution to the redshift. For the low redshift it could be expressed as  $z_{pec} = v_{pec}/c$ , where  $c$  is speed of light. In Fig. 1 (left) the impact of the peculiar velocities on the Hubble diagram is schematically shown.

To minimise the influence of peculiar velocities, in cosmological analyses a standard value of  $250 \text{ km s}^{-1}$  is added in quadrature to the redshift uncertainty [8]. It has nonetheless been observed that velocity dispersion can exceed  $1000 \text{ km s}^{-1}$  in galaxy clusters: the velocity dispersion equals  $1040 \text{ km s}^{-1}$  for the Perseus cluster [7] and  $1545 \text{ km s}^{-1}$  for ACO 2319 [6].

One can recalculate the velocity dispersion caused by the peculiar velocities to the magnitude uncertainty by  $\sigma_m = \frac{5\sigma_V}{cz \ln 10}$ . For instance, if a SN Ia host galaxy at redshift  $z = 0.05$  has a peculiar velocity of  $1040 \text{ km s}^{-1}$ , its contribution to the magnitude uncertainty will be  $\sigma_m \simeq 0.15 \text{ mag}$ . As it is seen from Fig. 1 (right), the magnitude uncertainty due to peculiar velocities of  $1000 - 1500 \text{ km s}^{-1}$  is greater than the intrinsic dispersion of  $\sigma_m \simeq 0.11 \text{ mag}$  for the scattering model C11 [9] in the PANTHEON analysis for the redshifts  $z < 0.15$  and,

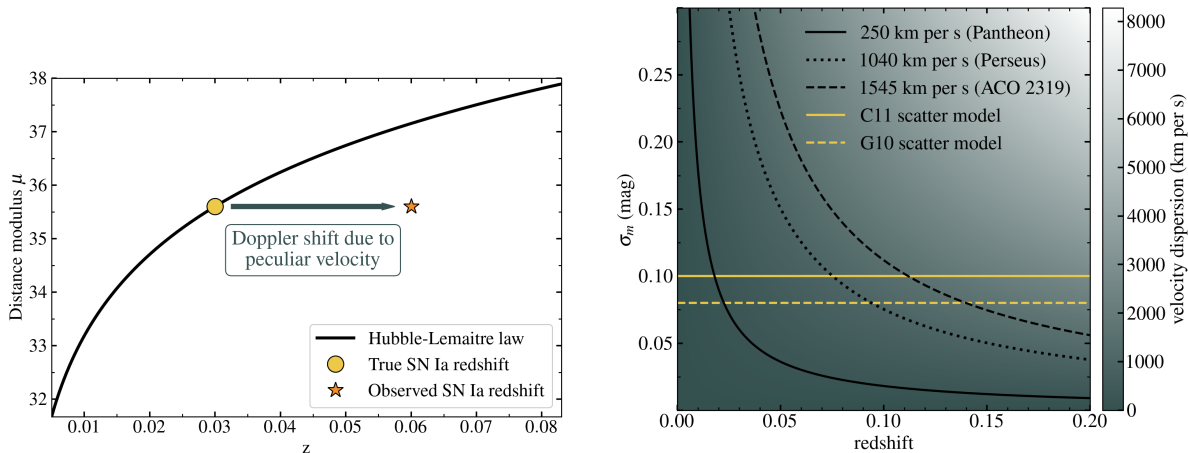


FIG. 1: Left: Shift caused by the redshift uncertainty due to peculiar velocity contribution  $z_{pec}$  on the Hubble diagram. Right: Redshift uncertainties due to peculiar velocities recalculated in magnitude units as a function of the cosmological redshift  $z$ . The solid black line corresponds to the uncertainties due to peculiar velocity correction applied in the PANTHEON analysis; the dashed and dotted lines correspond to ACO 2319 [6] and Perseus cluster [7] velocity dispersion, respectively. The contribution of peculiar velocities decreases with greater redshift.

therefore, has to be taken into account [10]. To decrease the contribution of this effect for those SNe that exploded in the galaxy clusters, we suggest to use the redshift of the clusters instead of the redshift of their host galaxies.

The similar analysis was performed for 11 Nearby Supernova Factory SNe Ia in galaxy clusters [11]. The authors showed that the Hubble residual dispersion of SNe Ia associated with galaxy clusters significantly decreased when the cluster redshift is taken as the cosmological redshift of supernovae. Our analysis applies the similar procedure to the PANTHEON cosmological sample of SNe Ia [8].

The paper is organised as follows. In Section II we present the PANTHEON data and used galaxy cluster catalogues. Section III describes the cross-matching procedure and the criteria of supernova search in the galaxy clusters. Finally, we conclude the paper in Section V.

## II. DATA

### A. Pantheon sample

As a supernova sample we use PANTHEON cosmological sample consisting of 1048 spectroscopically confirmed SNe Ia with redshift range  $0.01 < z < 2.3$ . This sample represents a compilation from several supernova surveys [8]. We choose this sample because it is one of the biggest intercalibrated samples of supernovae. Since the contribution of peculiar velocities is significant for the nearby Universe (see Fig. 1, right) we chose 297 SNe Ia from Pantheon sample with the redshifts  $z < 0.15$ .

### B. Galaxy clusters data

Galaxy clusters are characterised by the extremely hot gas in their centres that is observed as the diffuse X-ray emission [12, 13]. This observational fact can serve as the most effective and reliable way to establish which optically detected galaxy clusters are gravitationally-bound systems. Another observational appearance of hot gas in the central parts of clusters is the Sunyaev-Zel'dovich (SZ) effect that manifests as the distortion in the cosmic microwave background. Based on these effects we collect the following catalogues with galaxy clusters:

- MCXC which is the compilation of X-ray detected clusters of galaxies. This catalogue is based on publicly available ROSAT All Sky Survey-based, serendipitous cluster catalogues and finally comprises 1743 clusters [14].
- SWXCS which is the Swift X-ray Cluster Survey catalogue obtained using archival data from the X-ray telescope onboard the Swift satellite. The list of sources was cross-correlated with published optical, X-ray, and Sunyaev-Zel'dovich catalogues of clusters and 263 sources have been identified as clusters [15].
- XCS-DR1 which is the first data release from the XMM Cluster Survey. It consists of 503 detected X-ray clusters that were optically confirmed [16].
- Plank-SZ catalogue that consists of 439 clusters detected via their Sunyaev-Zel'dovich signal [17].

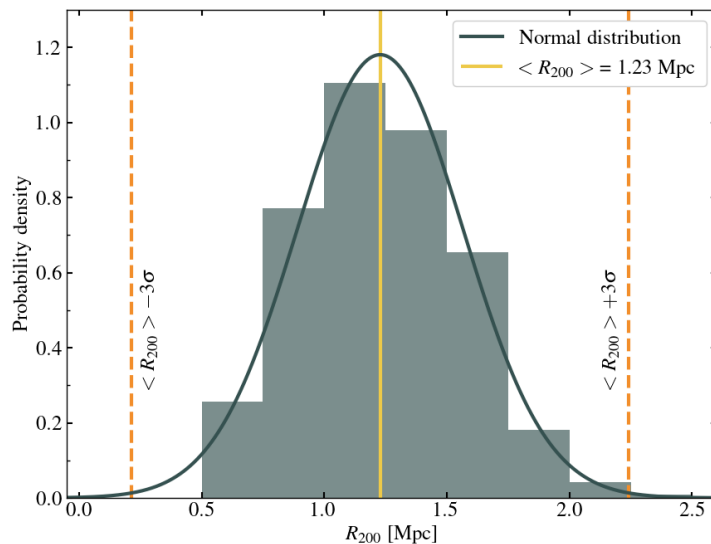


FIG. 2: Virial radius  $R_{200}$  distribution of galaxy clusters from MCXC [14]. The dark green solid line corresponds to the Gauss distribution of the clusters, the yellow solid line shows the mean  $R_{200}$  value, the yellow dashed lines present  $3\sigma$  area for this distribution.

### III. SEARCH OF SNE IA IN GALAXY CLUSTERS

#### A. Preliminary search

To find those PANTHEON SNe that belong to clusters of galaxies, we realise the cross-matching between the chosen cluster catalogues and PANTHEON sample. The preliminary search is performed in the cone of characteristic value  $R_{max}$ . To find  $R_{max}$ , we build the distribution of  $R_{200}$  parameter based on MCXC data, where  $R_{200}$  is the radius that encloses a sphere whose mean density is equal to 200 times of the critical density of the Universe (Fig. 2). The  $R_{200}$  parameter is calculated from  $R_{500}$  parameter from MCXC using the relation  $R_{200} \simeq 1.5R_{500}$ . After finding the mean value of  $R_{200}$  and its standard deviation  $\sigma_{R_{200}}$  we choose  $R_{max}$  criterion as  $R_{max} = \langle R_{200} \rangle + 5\sigma_{R_{200}} \simeq 2.92$  Mpc. Besides, for this preliminary search, we need to define some redshift cut. For the ACO 2319 cluster which demonstrates one of the highest value of velocity dispersion we calculate the maximum value of  $\Delta z = |z_{SN} - z_{cl}| \leq 5\sigma_{v_{pec}}/c \simeq 0.025$ . This value is used for the preliminary redshift cut. After applying both cuts, 30 SNe Ia in the galaxy clusters are identified by cross-matching procedure.

## B. Redshift of galaxy clusters

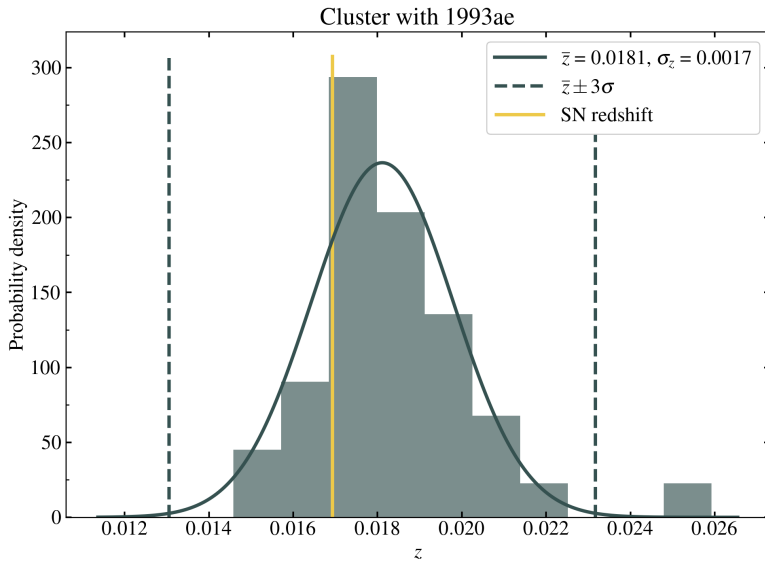


FIG. 3: The redshift distribution for galaxies inside the virial radius  $R_{200}$  of J0125.6-0124 cluster that hosts SN 1993ae. The supernova redshift given by PANTHEON is plotted by the yellow solid line. The dark green solid line corresponds to the Gauss distribution with the mean and the standard deviation values provided by the bi-weight technique. The dark green dash lines show  $3\sigma_z$  area.

To reduce the residuals on the Hubble diagram, we suggest in our analysis to use the galaxy cluster redshifts instead of the host galaxy redshifts for SNe Ia that belong to the clusters. To measure the cluster redshift, for each cluster we select all galaxies inside  $R_{200}$  radius around cluster centre that have the spectroscopic redshifts in SDSS<sup>1</sup> [18, 19]. Following [11] we choose the objects with the redshift value in the range  $z_{cl} \pm 5\sigma_V$ , where the cluster velocity dispersion  $\sigma_V$  could be found as  $\sigma_V \approx 10R_{200}H(z)$ ,  $H(z) = H_0\sqrt{(1 - \Omega_\Lambda)(1 + z)^3 + \Omega_\Lambda}$  for the flat Universe. For the resulting list of objects, we apply the bi-weight technique [20] and estimate the redshift values for 25 clusters. For example, the histogram with redshift distribution for one of the clusters is shown in Fig. 3. For other five clusters there are no data in SDSS, and we collect their redshifts from the SIMBAD database [21] and literature. Thus, we define the redshifts for all 30 galaxy clusters as well as their virial radii.

<sup>1</sup> <https://www.sdss.org>

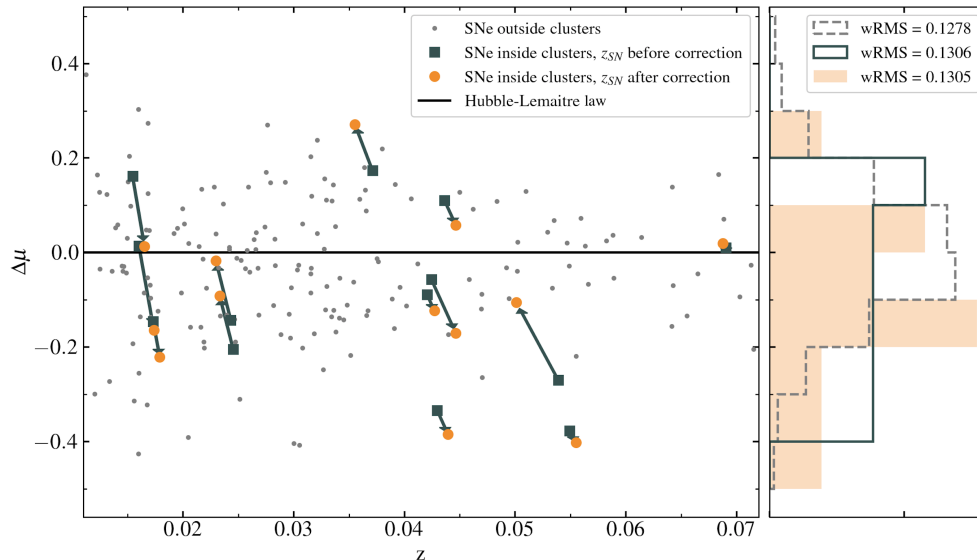


FIG. 4: Distance modulus residual on the Hubble diagram before peculiar velocity correction (dark green squares) and after it (orange circles). Hubble-Lemaître law is plotted by the black solid line based on the parameter values from [8].

### C. Final selection

After determining the redshift of galaxy clusters, we can perform the final selection to discard those supernovae that only projected near the clusters. Therefore, each SN has to satisfy the following conditions: I.  $|z_{SN} - z_{cl}| < 3\sigma_v/c$  and II.  $r < R_{200}$ , where  $r$  is a distance between supernova and galaxy cluster centre. These final cuts allow us to determine those PANTHEON SNe Ia that belong to the galaxy clusters. Table I presents the final list of 13 supernovae associated with clusters of galaxies and the main physical parameters of the clusters.

## IV. DISCUSSION

The effects of environment is another cause of uncertainties on the Hubble diagram. Using Pantheon data we consider the influence of environmental effects: the position of the SN relative to its host galaxy and the mass of the host galaxy – for supernovae in the field and supernovae in clusters, see Fig. 5. One can notice that host galaxies related with clusters are massive:  $\log_{10} M^{host}[M_{\odot}] > 10$ . Besides, SNe in clusters show even lower values of the

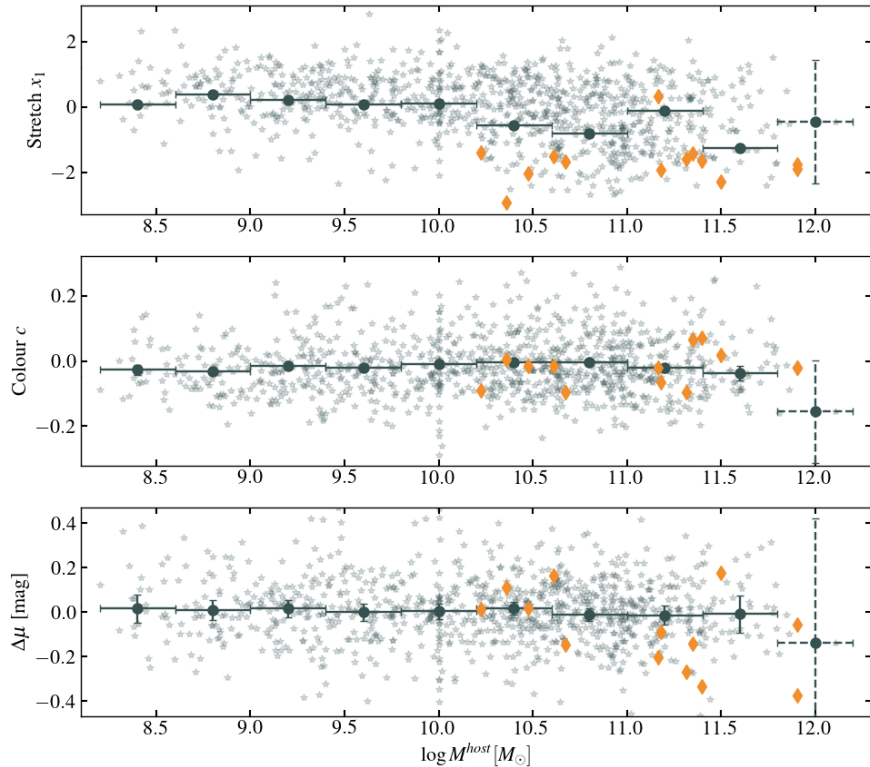


FIG. 5: The dependence of the parameters  $x_1$ ,  $c$  and  $\Delta\mu$  on the mass of the host galaxy for SN Ia from [8]. The bars illustrate the average values of the parameters for the selected mass range of host galaxies. SNe in clusters are shown with yellow rhombuses.

stretching parameter  $x_1$  in comparison with the average values that shown by green bars in Fig. 5 for each  $\log_{10} M^{host}[M_{\odot}]$  ranges. This effect may be due to the fact that in a cluster of galaxies it is more likely to detect elliptical host galaxies, which are characterized by large masses and lower values of the stretching parameter [22].

## V. CONCLUSION

Using the PANTHEON distance modulus values  $\mu_{obs}$  and the theoretical distance modulus for the flat  $\Lambda$ CDM cosmology [8], we found the distance modulus residuals for 13 SNe Ia in clusters. Then, we corrected the PANTHEON redshifts by the peculiar velocity correction found in Section III, and compared the Hubble diagram residuals before and after corrections (see Fig. 4). As expected, the supernova positions on the Hubble diagram do change. In perspective, we are going to evaluate the significance of the impact of the peculiar velocity

correction on the Hubble diagram. However, it can be already stressed that with increasing accuracy of the cosmological studies, such effects become more and more important and have to be taken into account.

### Acknowledgments

The authors are grateful to Pierre-François Léget for the helpful discussion. This work has made use of data from the Sloan Digital Sky Surveys [19] and the SIMBAD database, operated at CDS, Strasbourg, France [21].

### Funding

E.A.B. and M.V.P. acknowledge support from RSF grant 18-72-00159 and the Interdisciplinary Scientific and Educational School of Moscow University “Fundamental and Applied Space Research”.

### REFERENCES

- 
- [1] S. Perlmutter, G. Aldering, et al. *Astrophys. J.* , 517:565–586, June 1999.
  - [2] A. G. Riess, A. V. Filippenko, et al. *Astronomical Journal*, 116:1009–1038, September 1998.
  - [3] LSST Science Collaboration, Paul A. Abell, et al. *arXiv e-prints*, page arXiv:0912.0201, December 2009.
  - [4] P. F. Léget, E. Gangler, et al. *Astronomy and Astrophysics*, 636:A46, April 2020.
  - [5] Farhang Habibi, Shant Baghran, and Saeed Tavasoli. *International Journal of Modern Physics D*, 27(3):1850019, January 2018.
  - [6] D. Fadda, M. Girardi, et al. *Astrophys. J.* , 473:670, December 1996.
  - [7] J. A. L. Aguerri, M. Girardi, et al. *Monthly Notices of the RAS*, 494(2):1681–1692, March 2020.
  - [8] D. M. Scolnic, D. O. Jones, et al. *Astrophys. J.* , 859(2):101, June 2018.
  - [9] N. Chotard, E. Gangler, et al. *Astronomy and Astrophysics*, 529:L4, May 2011.
  - [10] Dragan Huterer. *arXiv e-prints*, page arXiv:2010.05765, October 2020.
  - [11] P. F. Léget, M. V. Pruzhinskaya, et al. *Astronomy and Astrophysics*, 615:A162, August 2018.

- [12] Elihu Boldt, Frank B. McDonald, et al. *Phys. Rev. Lett.* , 17(8):447–450, August 1966.
- [13] Craig L. Sarazin. *X-ray emission from clusters of galaxies*. Cambridge Astrophysics Series, Cambridge: Cambridge University Press, 1988.
- [14] R. Piffaretti, M. Arnaud, et al. *Astronomy and Astrophysics*, 534:A109, October 2011.
- [15] Teng Liu, Paolo Tozzi, et al. *Astrophysical Journal, Supplement*, 216(2):28, February 2015.
- [16] Nicola Mehrtens, A. Kathy Romer, et al. *Monthly Notices of the RAS*, 423(2):1024–1052, June 2012.
- [17] Planck Collaboration, Ade, P. A. R., et al. *A&A*, 594:A24, 2016.
- [18] J. C. Wilson, F. R. Hearty, et al. *Publications of the ASP*, 131(999):055001, May 2019.
- [19] SDSS-IV Collaboration, Romina Ahumada, et al. *Astrophysical Journal, Supplement*, 249(1):3, July 2020.
- [20] Timothy C. Beers, Kevin Flynn, and Karl Gebhardt. *Astronomical Journal*, 100:32, July 1990.
- [21] M. Wenger, F. Ochsenbein, et al. *Astronomy and Astrophysics, Supplement*, 143:9–22, April 2000.
- [22] M. V. Pruzhinskaya, A. K. Novinskaya, et al. *Monthly Notices of the RAS*, 499(4):5121–5135, December 2020.
- [23] John P. Huchra, Michael S. Vogeley, and Margaret J. Geller. *Astrophysical Journal, Supplement*, 121(2):287–368, April 1999.
- [24] Hitomi Collaboration, Felix Aharonian, et al. *Nature (London)* , 535(7610):117–121, July 2016.
- [25] H. Böhringer, W. Voges, et al. *Astrophysical Journal, Supplement*, 129(2):435–474, August 2000.

TABLE I: The final sample of PANTHEON SNe Ia in galaxy clusters. The 1st column contains SN names, the 2nd one — SN redshifts from the PANTHEON sample. The 3rd, 4th, 5th, and 6th columns contain the names of associated galaxy clusters, their coordinates from MCXC and redshift. Parameters  $R_{200}$  for each cluster are presented in the 7th column. The last column contains the references for the redshift  $z_{cl}$  source.

SN	$z_{SN}$	Cluster name	R.A. $_{cl}$	Dec. $_{cl}$	$z_{cl}$	$R_{200}$ [Mpc]	Ref.
2001ic	0.04296	J2310.4+0734	23 10 26.4	+07 34 37	0.0439	1.117	[18]
2003ic	0.05491	J0041.8−0918	00 41 50.1	−09 18 07	0.0555	1.840	[18]
2006al	0.06905	J1039.4+0510	10 39 27.9	+05 10 46	0.0688	1.225	[18]
2006gt	0.04362	J0056.3−0112	00 56 18.3	−01 13 00	0.0446	1.431	[18]
2006je	0.03712	J0150.7+3305	01 50 44.9	+33 05 24	0.0355	0.907	[18]
2008bf	0.02453	J1204.1+2020	12 04 11.6	+20 20 53	0.0233	0.727	[18]
2007nq	0.04243	J0056.3−0112	00 56 18.3	−01 13 00	0.0446	1.431	[18]
1994M	0.02431	J1231.0+0037	12 31 05.6	+00 37 44	0.0230	0.621	[18]
1999ej	0.01544	J0123.2+3327	01 23 12.2	+33 27 40	0.0165	0.761	[18]
2000dk	0.01602	J0107.4+3227	01 07 28.3	+32 27 43	0.0174	0.784	[18]
2005hf	0.04205	J0126.9+1912	01 26 54.5	+19 12 42	0.0427	0.519	[23]
2008L	0.0173	J0319.7+4130	03 19 47.2	+41 30 47	0.0179	1.954	[24]
1998dx	0.05389	J1811.0+4954	18 11 00.1	+49 54 40	0.0501	1.166	[25]